26 January 1968, Volume 159, Number 3813 SCIENCE

Solar X-rays

New observational techniques and refinements of theory are improving our knowledge of the sun's outer layers.

J. H. Underwood

Most of our knowledge about the sun has come from studies of the region of the solar spectrum between 3000 and 40,000 angstrom units (Å), in which 98 percent of the electromagnetic energy emitted by the sun lies. Radiation of wavelength shorter than 2900 angstroms is absorbed in the upper atmosphere and so cannot be observed with apparatus stationed at ground level. In recent years rockets and satellites have enabled us to extend our observations into the ultraviolet and x-ray regions, and it has been found that the spectrum extends at least to wavelengths of 1 or 2 angstroms. At even shorter wavelengths it is more convenient to characterize the radiation by the photon energy ϵ in thousands of electron volts (kev), the relation between wavelength λ (in angstroms) and energy ϵ being

$$\lambda = 12.3978/\epsilon$$

Photons with energies of 100 kev and more have been detected during flares.

The boundary between the x-ray and ultraviolet regions of the spectrum may be placed, somewhat arbitrarily, at 100 angstroms, as measurements below this wavelength require techniques different from those used at longer wavelengths. However, the study of the sun's shortwave emission has become an integral part of modern solar physics, one which is yielding important information about conditions in the sun's outer layers.

The author is on the staff of the Solar Physics Branch, NASA Goddard Space Flight Center, Greenbelt, Maryland.

Interest in the very-short-wavelength radiation from the sun was first associated with attempts to understand the region of ionized gas which exists above 70 kilometers in the earth's atmosphere—the ionosphere. The number of electrons per cubic centimeter at various levels in the ionosphere may be inferred from measurements on reflected radio waves. The early measurements seemed to indicate the presence of distinct strata in the ionosphere, which were termed the E layer, the F layer, and so on. However, rocket observations have shown that the normal ionosphere has a more or less continuous electron distribution, and that the "layers" are in fact due to large *gradients* of electron density. The density in the daytime E layer (or E region), which has its peak around the 105-kilometer level, is of the order of 10^5 electrons per cubic centimeter. In order to produce ionization in molecular oxygen, photons of at least 12.1-electron-volt energy are required; ionization of the other major atmospheric constituents requires even higher energies. Since electrons in the E region are being continuously lost by recombination, a continuous flux of short-wavelength radiation is required to maintain these electron densities. It was realized at a quite early stage in the study of the ionosphere that the photosphere, radiating like a black body at 6000°K, could not provide anything like the required amount of energy. In 1938 Hulburt (*1*) and Vegard (*2*) independently suggested that the sun emitted enough x-rays to produce the observed ionization. At about this time it was suspected that the temperature of the corona was very high, and a number of experimental and theoretical developments led to the gradual acceptance of this idea in the early 1940's. The most striking of these developments was the identification by Grotrian (*3*) and Edlén (*4*) of several of the mysterious coronal emission lines as forbidden transitions in highly ionized atoms of iron and other elements. Some of these lines had been known since the end of the last century and had previously defied attempts at identification. Other evidence for a high coronal temperature was provided by the Doppler widths of these lines, measured by Lyot (*5*) in 1932, and the detection of solar radio emission in the meter-wave region. The results indicated a temperature of around 10^6 °K, and in 1945 Shklovskii (*6*) showed that a corona at such a temperature could produce enough energy at short wavelengths to account for the electron densities observed in the ionosphere. Thus the stage was set for the first experiments carried out by the Naval Research Laboratory (NRL) from captured V-2 rockets, which led to the extension of observations of the solar spectrum into the ultraviolet, and for the first observation of solar x-rays by Burnight (*7*). Burnight's simple equipment consisted of Schumann plates (photographic emulsions containing very little ultraviolet-absorbing and x-ray-absorbing gelatin) which were exposed to the sun's rays through thin filters of aluminum and beryllium. When recovered and developed, the films showed blackening which could be attributed only to x-rays.

Experimental Methods

Since Burnight's initial observation, many experimenters, in several countries, have used a variety of rocket- and satellite-borne equipment to investigate solar x-radiation. A great deal of the pioneering work in this field

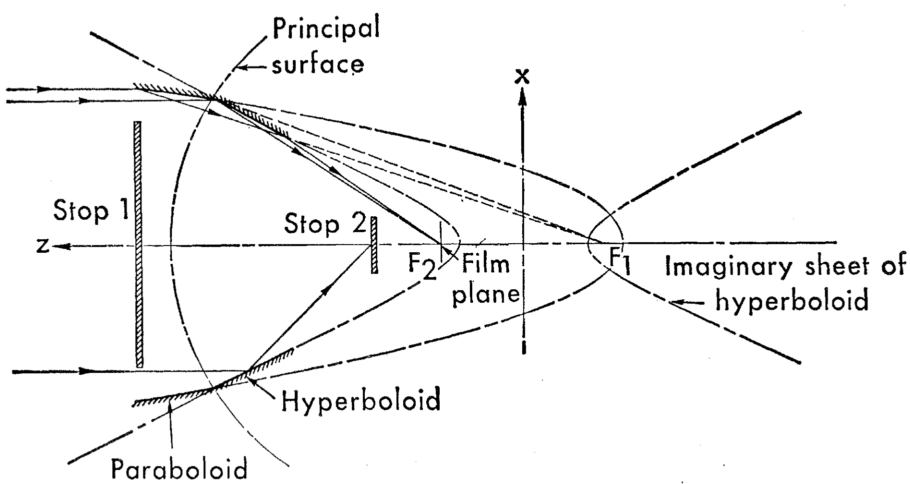

Fig. 1. Schematic diagram of a glancing-incidence x-ray telescope. The angles of glancing incidence have been exaggerated for clarity.

has been carried out by the Naval Research Laboratory.

For broad-band observations of the x-ray spectrum integrated over the whole solar disk, a number of instruments have been devised, including refined versions of Burnight's photographic equipment (*8*) and thermoluminescent photometers which employ materials such as manganese-doped calcium sulfate in the form of a powder. When such a substance is exposed to x-rays it absorbs energy which it can be made to reemit later (for example, after recovery from a rocket flight) in the form of visible light by heating in an oven. The total number of light photons emitted during the heating is proportional to the energy previously absorbed. Such a device has the advantage of being linear over a very large dynamic range. At present, however, the most popular techniques are based on the use of gas-filled detectors such as the mean-level ionization chamber and the pulse-counting proportional counter and Geiger counter, in conjunction with filters which define a broad wavelength band. Such detectors have been flown in rockets and satellites for almost two decades and have provided a wealth of data on the flux levels in the x-ray spectrum, on variability of the spectrum during the solar sunspot cycle, and on the x-ray emission from flares and other transient events. The ionization chamber measures the ion current produced in the detector gas by the incident x-rays. In order to convert this current into an energy flux, it is necessary to make some kind of assumption about the shape of the x-ray spectrum in the relevant wavelength region. Such an assumption is also necessary with the Geiger counter, which gives a pulse whose voltage is independent of the energy of the incident photon. On the other hand, a proportional counter produces a pulse whose voltage ("height") is proportional to the energy of the incident photon, and so this counter may be used to obtain crude information on the shape of the spectrum. However, the output pulses from such a counter show a considerable spread in height, even when the incident radiation is monochromatic. This effect is worst at the lower energies, and makes it necessary to exercise care in the interpretation of proportional-counter data. Normally the procedure used has been to assume that the x-ray spectrum may be represented by a Planckian "gray-body" distribution, or by a curve of the form exp $(-h\nu/kT_e)$, and by varying the temperature T_e obtain a fit to the experimental data. It is now clear, however, that most of the radiant energy at wavelengths below 25 angstroms originates as line emission, at least when no flare is occurring, so the validity of this continuum approach is doubtful. It appears necessary to reevaluate much of the earlier work done with broad-band photometers in terms of a spectrum dominated by line radiation.

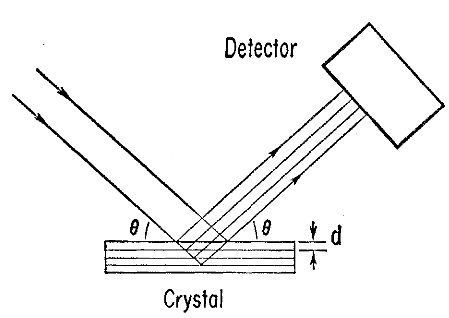

Fig. 2. Principle of operation of a Bragg crystal spectrometer.

Using gas-filled detectors mounted on several rockets fired during the course of an eclipse of the sun, members of the NRL group (*9*) were able to observe the occultation of different areas of the solar disk, and thus obtain information on the distribution of x-rays over the face of the sun. In addition, they measured the residual x-ray flux remaining at totality, a quantity which is important for the interpretation of E-region eclipse data. The same workers (*9*) were also the first to obtain an x-ray image of the sun, through use of a pinhole camera with an x-ray-sensitive emulsion. A thin aluminum-covered plastic foil over the pinhole served to exclude visible light and ultraviolet radiation outside the region of interest (below about 70 angstroms).

Recently a new technique for photographing the sun in x-rays has been developed. This relies on the fact, discovered by A. H. Compton in 1923, that x-rays can be reflected from polished surfaces at small angles of glancing incidence. For wavelengths around 10 angstroms, the glancing angle is about a degree. Following the work of Wolter (*10*), who showed how the aberrations, or optical defects, inherent in a glancing-incidence optical system might be overcome, reflecting telescopes for the x-ray region have been constructed and flown by Giacconi *et al.* (*11*) and by Underwood and Muney (*12*); these investigations have yielded promising results. Figure 1 shows the principle of one type of reflecting x-ray telescope, which is composed of a glancing-incidence paraboloidal primary element and hyperboloidal secondary element. Parallel rays from a distant object are reflected from each surface in turn and are focused at F_2 to form a real, inverted image on the film. Fairly thick filters may be used to isolate spectral bands, as this type of telescope is considerably faster than the pinhole camera; with the same filter, the glancing-incidence telescope requires only about 1/500 the exposure time needed for a pinhole camera. The image quality is good over a reasonably wide field of view, about 40 minutes of arc. Large glancing-incidence telescopes of this type, with a resolution of a few seconds of arc, will be carried on the first manned astronomical observatory in space—the Apollo Telescope Mount (ATM)—to obtain information on the structure and development of solar x-ray-emitting regions.

By placing a proportional counter or similar detector at F_2 and scanning the sun's disk, it is also possible to build up a picture of the spatial distribution of x-rays. An instrument of this type, constructed by American Science and Engineering, of Cambridge, Massachusetts, is now flying on the OSO-4 satellite, and is continuously mapping the sun in x-rays.

In order to understand the details of the atomic interactions involved in the production of solar x-rays, it is necessary to have information on the fine structure of the spectra. Below wavelength of 25 angstroms, the Bragg crystal spectrometer has so far proved to be the most useful type of high-resolution instrument. Figure 2 illustrates the principle. X-rays incident on the crystal are reflected from the planes of atoms only if the condition $n\lambda = 2d \sin\theta$ is satisfied. In this equation d is the distance between the atomic planes, θ is the angle between the incident rays and these planes, and n is an integer; normally the instrument is used with $n = 1$. It may be seen that, by rotating the crystal at a constant rate and the detector at twice this rate, one may sweep through the spectrum. In the region below 25 angstroms, crystals of potassium acid phthalate have been widely used. These have a $2d$ spacing of 26.6 angstroms. If a spectrometer is able to separate two features of a spectrum which are separated by a small wavelength interval $\Delta\lambda$ and which have a mean wavelength λ, then it is said to have a resolving power of $\lambda/\Delta\lambda$. A resolving power of about 1500 at 15 angstroms can be obtained with a good potassium acid phthalate crystal. The Bragg spectrometer may also be used in the region above 25 angstroms with crystals such as octadecyl hydrogen maleate ($2d = 63.5$ angstroms), or with built-up multilayers of soaps such as the metal stearates, which act as artificial crystals. However, with these techniques it is difficult to obtain a resolving power much greater than 150 in the longer-wavelength region, and in this part of the spectrum the glancing-incidence diffraction grating is likely to remain supreme.

It is also possible to obtain some spatial resolution with the Bragg crystal spectrometer, as two sources on the sun, separated by an angular distance $\Delta\theta$, will give two lines in the spectrometer for every line in their spectrum, provided $\Delta\theta$ is greater than the instrumental line width, which is determined mainly by the quality of the crystal used. In addition, the width of a spectral line from a source will give an indication of the size of the source. Blake *et al.* (*13*) used this property of the crystal spectrometer to distinguish lines originating in the whole corona from lines which came just from an active region.

The ultimate instrument for solar x-ray observation would be an "x-ray spectroheliograph" which could map the solar emission in one particular wavelength with high spatial resolution. It is possible that a combination of a glancing-incidence telescope and a Bragg crystal spectrometer will provide the solution in the near future.

Comparison of Experimental Results with Theory: The Quiet Sun

The x-ray emission from the sun can be conveniently divided into three components: (i) x-ray emission from the quiet corona—that is, emission at times

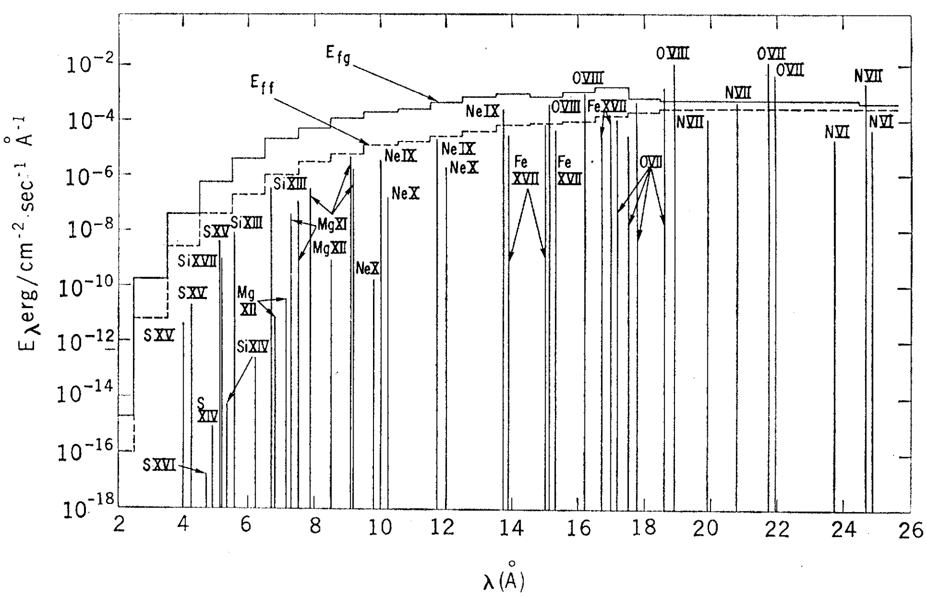

Fig. 3. Theoretical energy distribution in the solar spectrum at wavelengths below 25 angstroms, calculated for $T_e = 2 \times 10^6$ °K. E_{fg} (recombination radiation) and E_{ff} (bremsstrahlung) are summed in 1-angstrom intervals. [Mandel'stam (*17*)]

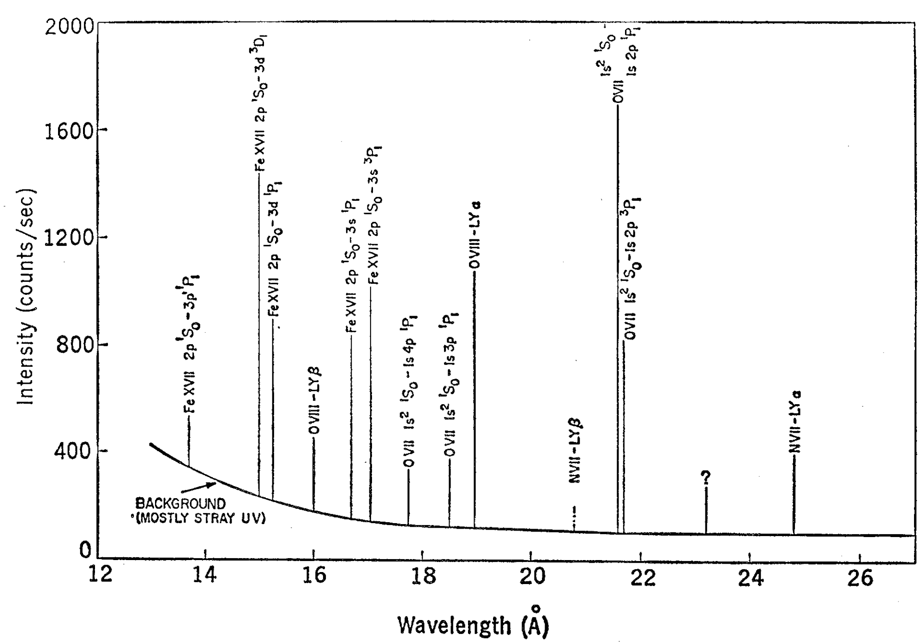

Fig. 4. X-ray spectrum of the sun obtained 25 July 1963 by Blake *et al.* (*13*).

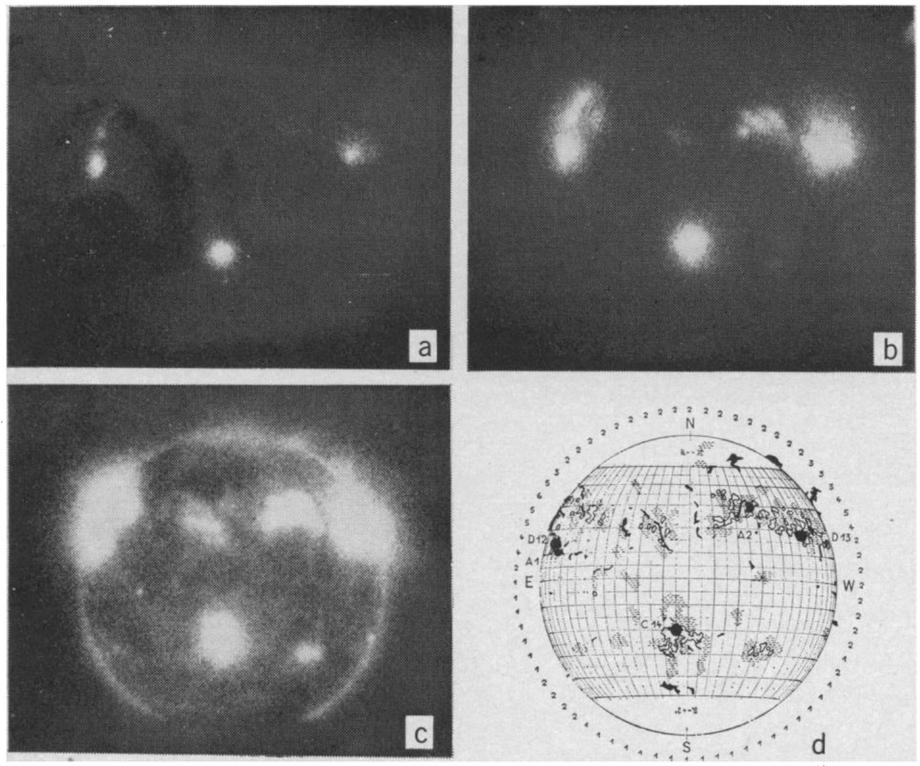

Fig. 5. X-ray photographs of the sun obtained on 20 May 1966. (a) Wavelength region 3–11 angstroms; (b) wavelength region 8–20 angstroms; (c) wavelength region 27–40 angstroms (contaminated by some radiation at 3–11 angstroms); (d) Fraunhofer Institut map of the sun for the same day.

of no solar activity, or from the undisturbed areas of the corona far from active regions; (ii) a slowly varying component from more or less long-lived active regions in the corona above sunspots, plages, and so on, which shows a 27-day period due to the apparent motion of the active regions caused by the solar rotation; (iii) rapidly varying x-ray bursts, sometimes, but not always, associated with visible transient phenomena such as flares or eruptive prominences, or radio bursts.

In order to compute theoretically the x-ray spectrum expected from the solar corona we must, essentially, determine the number of atomic transitions of different kinds taking place per second in a unit volume of the hot gas. To do this we need to know (i) the abundance of the various chemical elements in the corona; (ii) the state of ionization of each of the elements at the temperature of the gas; (iii) the number of interactions per second between the ions and the electrons leading to the emission of x-ray photons; and (iv) the amount of radiation lost by reabsorption in the gas.

The quiet corona is a high-temperature plasma ($T \sim 1.5 \times 10^6$ °K) of low density relative to typical laboratory plasmas. In the lower corona, some tens of thousands of kilometers above the surface of the photosphere, the electron density is around 5×10^8 electrons per cubic centimeter; this density decreases rapidly with height. The relative abundances of the elements in the corona are on the whole the same as the relative abundances in the photosphere, although there is evidence that some of the heavier elements—iron in particular—have an anomalously high abundance in the corona. This question will undoubtedly be resolved when further accurate measurements of emission-line intensities in the far-ultraviolet and x-ray regions become available (see *14*).

The state of ionization of any element is determined by the balance between (i) processes leading to ionization and (ii) recombination processes. The most important process by which atoms become ionized is inelastic collision of an atom with an energetic electron; the energy lost by the electron serves to strip another electron off the atom. The ion thus formed may lose another electron in a further collision, and so go stepwise to higher and higher stages of ionization. Very high stages of ionization are observed in the corona. The first line emission from the corona ever to be observed—the "green line" at 5303 angstroms—belongs to the 14th spectrum of iron, Fe XIV. This is the spectrum of iron which has been ionized 13 times (Fe I is the spectrum of neutral iron).

A colliding ion and electron may recombine if the conditions of the impact are right. The excess energy may be emitted in the form of a photon. This photorecombination is one of the two important processes by which atoms return to lower stages of ionization. The other, known as dielectronic recombination, may take place if an ion collides with an electron which has sufficient energy to raise *two* electrons to excited levels. The ion and electron combine to form this doubly excited state, which may then fall rapidly to a lower state of excitation with the emission of photons, so that the new electron ends up firmly bound to the ion.

The recent recognition by Burgess (*15*) of the importance of this recombination process for certain elements has helped to put the theory of the ionization balance of the corona on a much sounder basis. It has helped to explain a long-standing discrepancy between the ionization temperature of the corona as deduced from measurements of intensity ratios of forbidden lines in the visible region and the temperature as determined by other means, such as measurements of the Doppler widths of the lines.

If the rates of ionization and recombination are known, we may assume equilibrium and write

$$N_{z+1}/N_z = q_z/\alpha_z$$

where N_z is the number density of ions with charge z; q_z is the ionization rate for this ion; and α_z is the rate at which ions with charge $z + 1$ recombine to form ions with charge z. Thus the coronal population of each kind of ion may be obtained; note that the state of ionization does not depend on the density but depends only on the temperature.

The computation of the soft x-ray spectrum produced by this ionized plasma takes into account three processes. The more important of the three are (i) line radiation due to allowed transitions of outer ("optical") electrons of the ions, which, under the conditions prevailing in the quiet corona, are excited mainly by collisional excitation, and (ii) continuous emission due to free-bound (recombination) transitions between the states of the continuum and bound levels. The third process, free-free radiation or bremsstrahlung, also makes a small contribution to the continuous spectrum. Calculations have been made by a number of workers, notably G. Elwert (*16*). Figure 3 is a spectrum of the region below 25 angstroms, computed by Mandel'stam (*17*). It may be seen that most of the x-ray flux in this region is expected to be from recombination and line radiation from carbon, nitrogen, oxygen, neon, and other, heavier elements. The integrated energy flux in the 2- to 8-angstrom region is calculated to be 5×10^{-5} erg cm^{-2} sec^{-1}. This value agrees well with the value obtained by Pounds (*17*) near the minimum of solar activity.

So far, the only high-resolution observation of the solar spectrum in the region below 25 angstroms to be made under relatively quiet solar conditions has been that of Blake *et al.* (*13*), who used a Bragg crystal spectrometer with a potassium acid phthalate crystal. Even so, on the day this spectrum was obtained there was a small active region on the sun. The lines emitted from the whole corona could, however, be distinguished from those emitted only by the active region by their greater apparent breadth, as mentioned above. The spectrum, which is reproduced in Fig. 4, shows many of the lines predicted for this region. However, because of the low sensitivity of this type of spectrometer to continuous radiation, and the difficulty of reducing scattered ultraviolet radiation in the instrument, it was not possible to obtain information on the intensity of the continuous spectrum.

Emission from Active Regions

The sun is very rarely completely "quiet"; even at sunspot minimum there are usually one or two small active areas visible in the Hα line of hydrogen or the K line of calcium. At sunspot maximum these regions may be large and numerous. The enhanced radio and x-ray emission associated with a sunspot group or plage area comes from a region of enhanced density and temperature located above it in the corona. Above a "typical" active region the density may be enhanced by a factor of 2 to 5. However, if a "permanent coronal condensation" appears, the temperature inside it can be 4 to 5×10^6 °K, and the electron density, 10^{10} to 10^{11} electrons per cubic centimeter. Such condensations are visible on eclipse photographs as local brightenings in the white-light corona, and usually show the line of Ca XV at 5694 angstroms—a line which indicates a high temperature (814 electron volts are required to produce 14-times-ionized calcium).

Computation of the x-ray spectrum of an active region can be carried out on the same lines as computation of the x-ray spectrum of the quiet corona if the temperature, density, and emitting volume are known. For very dense regions, reabsorption of the radiation in the emitting region may have to be taken into account.

Figure 5 shows a set of x-ray photographs of the sun that W. S. Muney and I obtained on 20 May 1966, using a glancing-incidence telescope of the type shown in Fig. 1, which was flown in an Aerobee rocket. A Fraunhofer map of the sun for the same day is shown for comparison. For Fig. 5a a filter of beryllium 0.076 millimeter thick was used. It may be seen that the emission in the wavelength band (3–11 angstroms) transmitted by the filter-telescope combination is confined to three fairly small areas over the main active regions. At these places there must be a continuous flow of energy into the corona in order for the observed high-energy emission to be maintained. Because the x-rays are emitted in a region quite high above the

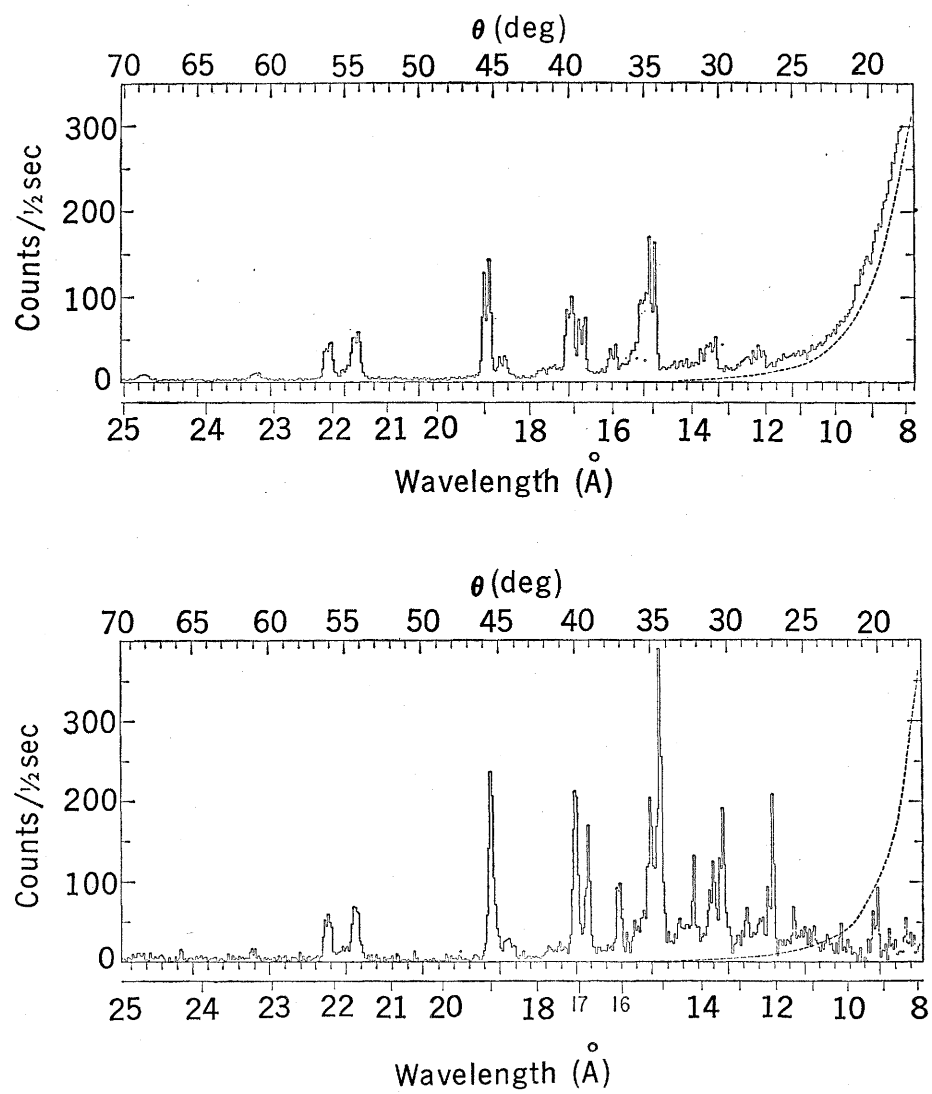

Fig. 6. X-ray spectra of the sun at wavelength below 25 angstroms, obtained by the OV1-10 satellite [reproduced courtesy of A. B. C. Walker and H. Rugge (*18*)]. (Top) Spectrum obtained on 30 December 1966; (bottom) spectrum obtained on 23 February 1967, a short time after a medium-sized flare had occurred. The dotted line shows the estimated background due to scattered ultraviolet radiation; this has been subtracted in the spectrum at bottom.

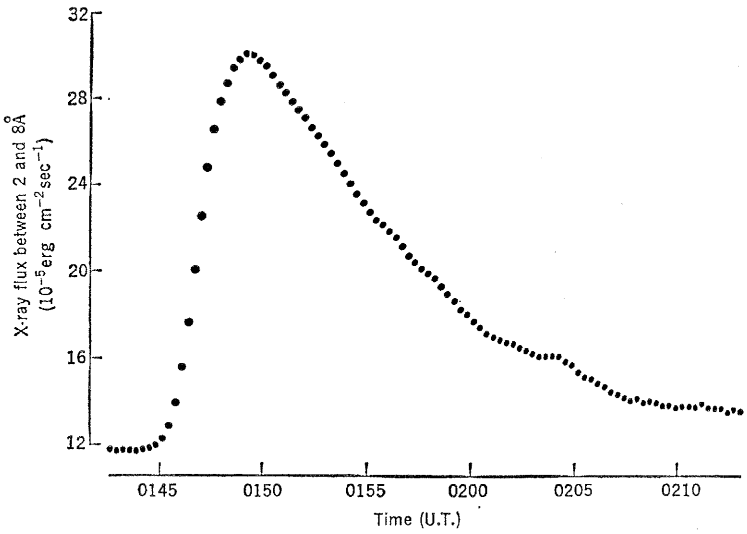

Fig. 7 (above). X-ray burst recorded 8 March 1962 by ion chambers aboard satellite OSO-1.

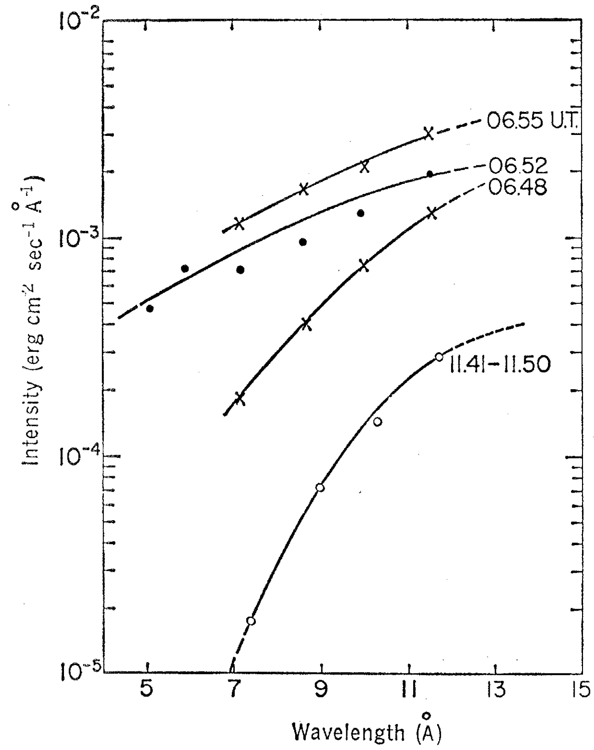

Fig. 8 (right). Proportional-counter flare spectra obtained by the Ariel 1 satellite on 3 May 1962, during a class-2 flare (*20*).

surface of the photosphere, one also sees on the northeast limb the emission associated with a plage group which is still on the invisible side of the sun and does not rotate into view until a day or two later.

For Fig. 5b a 5-second exposure and an aluminum foil 0.0064 millimeter thick were used. The transmission band of this filter is 8–20 angstroms, and it may be seen that, at these wavelengths, the "x-ray plages" have a definite size and shape, corresponding rather closely to the bright calcium regions. Finally, for Fig. 5c a 30-second exposure and a titanium filter 0.0022 millimeter thick were used. This filter has roughly the same transmission characteristics as the beryllium filter, plus a second pass-band at 27–40 angstroms. At these wavelengths every plage region, down to the very smallest, can be seen to have an associated x-ray emission. Details as small as 20 seconds of arc in diameter can be seen in this photograph. There is also a general emission from the undisturbed regions of the corona which shows limb brightening, indicating that the quiet corona is optically thin for radiation of this wavelength. An interesting phenomenon is the total absence of limb brightening over the south pole. This indicates that the electron density over the polar region is considerably less than that at lower latitudes, a rather abrupt transition taking place at a latitude of about 60 degrees. The corresponding region around the north pole does not show a similar darkening but is occupied by a "tuft" of emission, seemingly unassociated with underlying plage.

At present, high-resolution spectra in the region below 25 angstroms are being obtained by instrumentation aboard NASA's third Orbiting Solar Observatory. Previously, the small satellite OV1-10 of the U.S. Air Force had obtained similar spectra. The sunspot cycle is at present in the ascending phase, and the spectra being obtained are typical of a fairly active sun. Figure 6 (top) is a spectrum obtained by Walker *et al.* (*18*) on 30 December 1966. It shows the same lines that were seen by Blake *et al.* (Fig. 4) under quieter conditions, but, in addition, there appear lines of even more highly ionized species such as Fe XVIII and Ni XIX, indicating once more the very high temperature of the active regions.

Transient X-ray Events

In addition to the slow variation of x-ray flux seen as active regions are born and die away, and rotate on and off the visible face of the sun, rapidly varying x-ray events are frequently seen. Many of these events are associated with chromospheric flares or eruptive prominences, but a large number have no counterpart in the visible region of the spectrum. Zhitnik *et al.* (*19*) managed to photograph, with a pinhole camera, a sudden x-ray event which occurred in a part of the corona which had no underlying active region visible in the Hα line or the K line of calcium. Even for those events which do occur in conjunction with a flare, the correlation between the intensity of the burst and the importance of the flare, and between the time of maximum x-ray emission and the peak of Hα-line intensity, are rather poor.

The characteristics of a typical x-ray burst are the rather rapid enhancement of the x-ray flux, especially at the shortest wavelengths (hardening of the spectrum), which is followed by a more gradual fall. Figure 7 shows the variation of the flux recorded by ion chambers aboard the OSO-1 satellite during a small event on 8 March 1962. The data were analyzed on the assumption of a 2.8 $\times$ 10^6 °K black-body spectrum. Figure 8 shows spectra obtained during the course of a class-2 flare on 3 May 1962, by proportional counters aboard the Ariel 1 satellite. The "hardening" of the spectrum is clearly visible (*20*).

Only recently have high-resolution spectra of flares at wavelengths below 25 angstroms been obtained. Figure 6 (bottom) is a spectrum obtained by the Aerospace Corporation group a short while after the occurrence of a moderate-sized flare. It may be seen that a large number of new lines make their appearance during flares, many of them due to transitions in very highly ionized states of iron and nickel. Many of the weaker lines have not yet been identified.

Neupert *et al.* (*21*) have recently obtained spectra of flares at wavelengths down to 1 angstrom. A prominent feature of these spectra is the appearance of a number of lines in the 1.3- to 3.0-angstrom region. Figure 9 shows the spectrum of a typical flare, with some tentative line identifications. The strong line marked Fe at 1.86 angstroms is the $1s^2$–$1s2p$ line of the Fe XXV spectrum, which is characteristic of iron atoms which have been stripped of all but two of their electrons. The spectrum is therefore similar to that of neutral helium, although the lines appear at a much shorter wavelength than they do in the helium spectrum. The 1.86-angstrom line is probably blended with x-ray lines due to inner shell transitions in less highly ionized species of iron. The lines at 1.60 and 2.19 angstroms are the analogous helium-like lines of the Ni XXVII and Cr XXIII spectra. These transitions have recently been observed in the laboratory, in the spectra of energetic vacuum sparks (*22*).

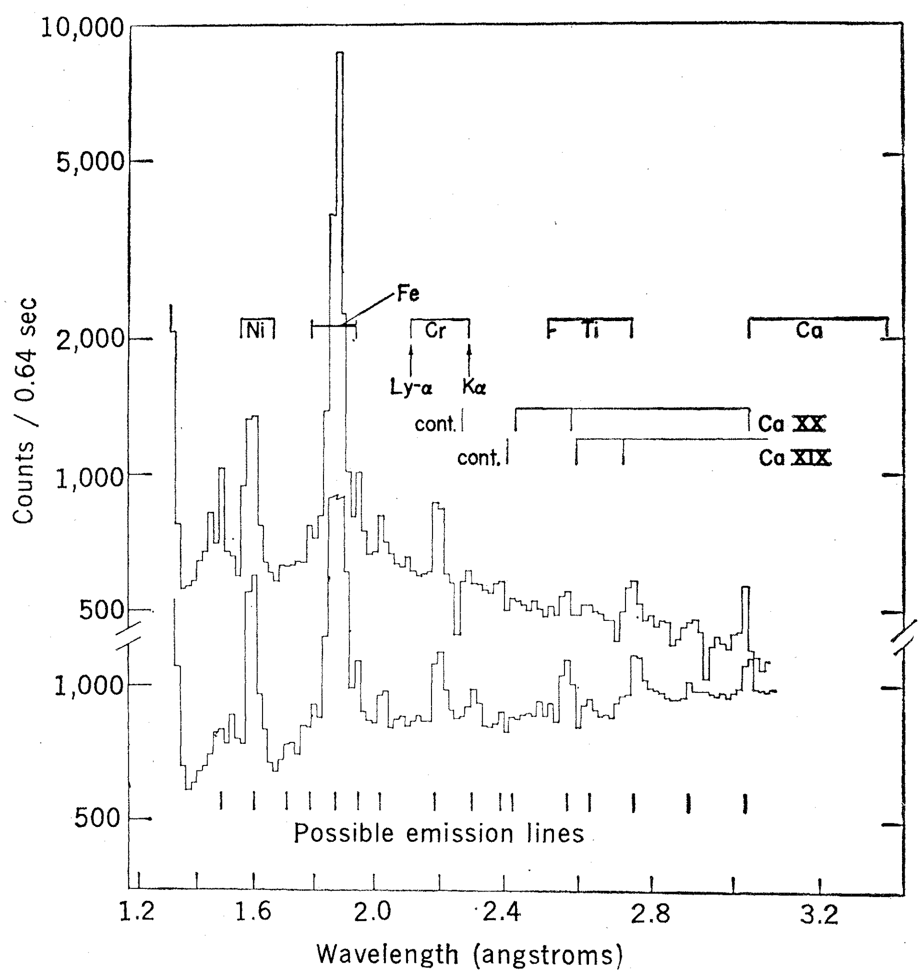

Fig. 9. Spectrum of the 1.3- to 3.1-angstrom region obtained during a flare on 22 March 1967 by instrumentation aboard satellite OSO-3. [Reproduced courtesy of W. M. Neupert]

The production of such high stages of ionization and of hard x-ray photons requires a source of high-energy electrons. For instance, in the laboratory spark work mentioned above it was found that 19,000 volts across the spark electrodes were needed to excite the Fe XXV spectrum. An early piece of evidence for the existence of high-energy photons in solar flares was provided by Chubb *et al.* (*23*), who observed a flux of high-energy photons from a flare, whose energies extended up to 100,000 electron volts. These workers showed that the spectrum was equivalent to that expected from a thermal plasma with a temperature of the order of 10^8 degrees. However, one must also take into account the possibility that the radiation is nonthermal, produced by beams of electrons which are somehow accelerated to high energies within a relatively cool but dense mass of plasma, and that the radiation at high energies could be produced not only by bremsstrahlung but also by processes such as synchrotron radiation and the inverse Compton effect. Further studies of hard solar x-rays will be required to resolve these questions. It is likely that x-ray studies will provide a significant insight into the mechanism of flares.

Effect of X-rays on the Ionosphere

I mentioned above that x-rays are a contributing factor in the ionization of the upper atmosphere. The wealth of data accumulated on solar x-rays over the past years has led to a much better understanding, both qualitative and quantitative, of the effects of these rays on the lower ionosphere. The most spectacular phenomena occur during flares, when the flux in the spectral region between 2 and 8 angstroms can rise by a factor as large as 10^5, resulting in a large increase in electron density in the 50- to 100-kilometers, or D, region of the ionosphere. Long-distance radio-wave propagation is severely affected by these changes in ionization. In most cases the signal strength becomes severely attenuated, in which case the event is termed shortwave fadeout.

The role of the less spectacular variations in x-ray flux due to the slowly varying component and to solar-cycle variations in the formation of the lower ionosphere is less clearly understood and still under study. If any substantial progress with this complex problem is to be made, it appears imperative that measurements on the physical and chemical condition of the lower ionosphere be made simultaneously with observations of the solar x-ray spectrum, with the techniques described above. Continuing observations of solar x-rays may be expected to lead to an improved understanding of the physical processes occurring in the earth's lower ionosphere and the sun's outer atmosphere.

References and Notes

1. E. O. Hulburt, *Phys. Rev.* **53**, 344 (1938).
2. L. Vegard, *Geophys. Pub.* **12**, 5 (1938).
3. W. Grotrian, *Naturwissenschaften* **27**, 214 (1939).
4. B. Edlén, *Z. Astrophys.* **22**, 30 (1942).
5. B. Lyot, *ibid.* **5**, 73 (1932); *Astronomie* **51**, 203 (1937).
6. I. S. Shklovskii, *Dokl. Akad. Nauk SSSR* **64**, 37 (1949).
7. T. R. Burnight, *Phys. Rev.* **76**, 165 (1949).
8. K. A. Pounds and P. J. Bowen, *Monthly Notices Roy. Astron. Soc.* **123**, 348 (1962).
9. T. A. Chubb, H. Friedman, R. W. Kreplin, R. L. Blake, A. E. Unzicker, *Mem. Soc. Roy. Sci. Liege* **4**, 228 (1961).
10. H. Wolter, *Ann. Physik* **10**, 94 (1952); *ibid.*, p. 286.
11. R. Giacconi *et al.*, *Astrophys. J.* **142**, 1274 (1965).
12. J. H. Underwood and W. S. Muney, *Solar Phys.* **1**, 129 (1967).
13. R. L. Blake, T. A. Chubb, H. Friedman, A. E. Unzicker, *Astrophys. J.* **142**, 1 (1965).
14. A. K. Dupree and L. Goldberg, *Solar Phys.* **1**, 229 (1967).
15. A. Burgess, *Astrophys. J.* **139**, 776 (1964); *ibid.* **141**, 1588 (1965).
16. G. Elwert, *J. Geophys. Res.* **66**, 391 (1961).
17. See S. L. Mandel'stam, *Space Sci. Rev.* **4**, 587 (1965); this paper is an excellent review of the whole subject of solar x-rays.
18. A. B. C. Walker, H. R. Rugge, W. T. Chater, C. K. Howey, *Trans. Amer. Geophys. Union* **48**, 151 (1967).
19. I. A. Zhitnik, V. V. Krutov, L. P. Malyavkin, S. L. Mandel'stam, G. S. Cheremukhin, *Kosmicheskie Issled.* **5**, 276 (1967); see also S. L. Mandel'stam, *Appl. Opt.* **6**, 1834 (1967).
20. J. L. Cullhane, A. P. Willmore, K. A. Pounds, P. W. Sanford, *Space Res.* **4**, 741 (1964).
21. W. M. Neupert, W. Gates, M. Swartz, R. Young, *Astrophys. J.* **149**, 79 (1967).
22. L. Cohen, U. Feldman, M. Swartz, J. H. Underwood, in preparation.
23. T. A. Chubb, R. W. Kreplin, H. Friedman, *J. Geophys. Res.* **71**, 3611 (1966).

Uptake of Protein by Mammalian Cells: An Underdeveloped Area

The penetration of foreign proteins into mammalian cells can be measured and their functions explored.

H. J.-P. Ryser

More than 20 years have elapsed since Avery, MacLeod, and McCarty published the first observation of genetic transformation in pneumococci (*1*). This discovery, once confirmed and broadened (*2*), initiated the search for similar phenomena in cells of higher organisms. It prepared the way for major discoveries such as the initiation of infection (*3*) and malignant transformation (*4*) in mammalian cells by means of nucleic acids extracted from infectious or oncogenic viruses. Efforts to achieve genetic transformation in animal cells led to several claims of success (*5*), and although results on this subject have been difficult to reproduce, they have at least suggested that genetic transformation of animal cells is within reach.

There is no need to point out the implications of this line of research. One of its secondary benefits, however, deserves to be emphasized. By giving us the first definitive demonstration that macromolecules can exert specific biological effects in host cells, these investigations have changed our understanding of membrane function. They have compelled cell biologists to recognize that the study of membrane transport is no longer restricted to the diffusion and the active transport of small solutes but must reckon with the penetration of macromolecules.

Mechanisms that can account for this type of transport were proposed more than 10 years ago (*6*), and there is now near-consensus among cell biologists that macromolecules are drawn into cells by membrane movements associated with vesicle formation. The process is generally described as endocytosis or, depending on its dimensions, as micropinocytosis, pinocytosis, or phagocytosis. It is believed that endocytotic vesicles or vacuoles containing foreign macromolecules receive intracellular digestive enzymes by fusing with lysosomes (*7*). The largest part of the ingested macromolecules, it is assumed, undergoes intracellular digestion, whereas a smaller fraction escapes destruction and finds access to specific sites of action. The smallest vesicles containing ingested macromolecules are of the order of 0.05 micron in diameter and are seen only with the electron microscope. Larger vesicles, however, are visible with the light microscope, and several semiquantitative studies of pinocytosis have relied on the simple enumeration of such vacuoles (*8*). Because the quantitative evaluation of electron-microscopic data must contend with considerable difficulties and limitations, there is today a remarkable abundance of morphological data contrasting with a dearth of reliable quantitative studies of endocytosis. The emphasis on morphological aspects may explain why the biologists committed to the traditional study of transport fail to be captured by this problem. The sequence of vesicle formation, migration, and fusion and the superimposed process of digestion is altogether too complex to lend itself to a mathematical analysis of transport kinetics. On the other hand, virologists, who care about the ultimate biological function of a foreign macromolecule, tend to neglect the physiology of uptake and seldom consider this initial step as a subject worthy of special investigation. These may be some of the reasons why, 20 years after Avery's momentous discovery, little has become known about the physiology of macromolecular transports across animal cell membranes.

Selection of a Model and Technical Stumbling Blocks

Investigators measuring the uptake of macromolecules face a few technical problems which, on occasion, must have seemed so elementary that they were ignored. One of them is the distinction between adsorption and uptake. Macromolecules tend to be adsorbed heavily to the surface of living cells. The process is rapid, complete within seconds, and reversed by repeated washing. It shows little or no dependence

The author is assistant professor of pharmacology at Harvard Medical School, Boston, Massachusetts.